Abdulkadir Mohammed Noori Jassim et al /J. Pharm. Sci. & Res. Vol. 11(3), 2019, 1025-1034

ISSN:0975-1459
Journal of Pharmaceutical Sciences and Research
www.jpsr.pharmainfo.in

Green Synthesis of Silver Nanoparticles Using *Carica Papaya* Juice and Study of their biochemical application

[1*]Abdulkadir Mohammed Noori Jassim, [1]Mustafa Taha Mohammed, [2]Safanah Ahmed Farhan, [2]Rasha Moniem Dadoosh, [2]Zainab Naeif Majeed, [1]Ahmed Mutanabbi Abdula

[1]Chemistry Department, College of Science, Mustansiriyah University. Iraq.
[2]Polymer research unit, College of Science, Mustansiriyah University, Iraq.

Abstract

The nanoparticle synthesis by green method has great concern to many researchers' to find new biomedical and pharmaceutical material. In this study, an eco-friendly method used for producing silver nanoparticles (AgNPs) utilizing *Carica Papaya* fruit juice as a reducing and stabilizing laborer.

Various optimum conditions to producing AgNPs are studied and the synthesized NPs are identified by UV-Vis, FT-IR, AFM, SEM and Zitasizer. Particle size (40-105nm) is indicated by AFM and SEM with average diameter 75.68nm and spherical in shape, while DLS showed the coated particle size with 555.21nm. The fruit juice showed many elements and compounds which analyzed by AAS, GC-Mass, respectively. So, the information appeared that fruit juice can work as a good bio-reductant to produce AgNPs, with the acceptable role as antibacterial agent and could be effective factors against different enzymes.

Key words: Green synthesis, Silver nanoparticles, *Carica Papaya*, Enzyme and Bactericidal effect

INTRODUCTION

Nanotechnology includes the manufacture, characterization and/or manipulation of components that have approximately 1-100 nm in length in one its dimension. When particle size is decreased lower than this dimension, the resulting materials appear chemical and physical properties differ greatly from macro scale components [1]. The metallic nanoparticles (NPs) have many implementations in different field like cosmetics, coating, electronics, packaging, also in biotechnology [2]. The NPs can pass blood vessels and moving toward target organ, this allow for new imaging, therapeutic and bio-medical implementations [3].

The effectiveness of AgNPs is come from teeny size. These NPs possess huge surface area prorated to its volume. Nanomaterials are rapidly developing areas of nano-medicine and bionano-technology. Moreover, it has interesting physicochemical properties [4, 5]. A tiny quantity of silver is too safe for cells in human, while it lethal to microorganisms [5]. Green synthesis of NPs by eco-friendly way is accomplished by diverse biological entities like plant extracts, yeast and bacteria [6].

It is worth mentioning that the NPs fabrication utilizing plants presents significant advantages over other biological methods [7].

Papaya, Papaw Kates and Paw Paw are the major commonly name for *Carica papaya* (*C. papaya*), one of the medicinal plants, belongs to family Caricaceae, which are used since long time ago to treat various diseases [8, 9].

Many researches deals with *Carica papaya* fruit extract on rat indicate, the antioxidant and immunostimulant feature versus acrylamide toxicity [10]. The leaves and fruit extracts containing many proteolytic enzymes, phenols and vitamins, which acts as excellent antimicrobial and good antioxidant agent [11].

Our study aimed to investigate the chemical components of the *Carica Papaya* Juice and synthesis, characterization of AgNPs using this juice without external addition of capping agent, surfactant or reducing agent, with investigate the influence of various conditions to producing AgNPs. The efficacy of the synthesized AgNPs as antibacterial agent, with its effect against GOT and GPT enzymes were investigated.

MATERIALS AND METHODS

1. Materials

Silver nitrate AgNO3 was supplied from Sigma–Aldrich and other reagents used in the reaction were of analytical grade with maximum purity. Throughout the experiment deionized water was used in all work.

2. Chemical detection of the plant components:

The chemical components (glycosides, alkaloids, saponins, phenolic compounds, tannins, resins, flavonoids and proteins) of the *Carica papaya* juice were detected [12].

3. Atomic absorption analysis:

The trace elements of the *Carica papaya* juice and the AgNPs concentration were mesured using Flame Atomic Absorption Spectroscopy (AA-680, Shimadzu-Japan). Standard solutions were prepared for each element and the absorbance values of these samples were determined from the calibration curve.

4. GC-Mass analysis:

Four milliliter of *Carica papaya* juice was taken, centrifuged, filtered and extracted by ethyl acetate (4 x 20) using separating funnel. The obtained EOAc portion was collected, concentrated by evaporating under vacuum at 50ºC using the rotary evaporator and then GC-Mass (QP2010Ultra, Shimadzu Co., Kyoto, Japan) analysis was performed [13].

5. Preparation of the *C. Papaya* fruits:

The *Carica papaya* fruit were obtained from the china market. The fruits were washed many times. The juice was obtained via pressing the fresh fruit through the gauze after excluded the seed. Then, it was filtered then centrifuged for ten min. (2500 rpm). The juice kept frozen at -20ºC until used.

6. Biosynthesis of silver nanoparticles

The *Carica papaya* juice (10 ml) was gathered with 10 ml of 1 mM $AgNO_3$ in round bottom flask connected with condenser and the solution was keep stirred. The bio-reduction of the Ag^+ in this reaction was affirmed by alteration in color: ($AgNO_3$) no color to ($AgNO_3$+juice) yellowish color to bright yellow color, then to dark brown. The solutions were then stored at 4°C in dark glass bottles.

7. Fixation of various parameters

7.1. Temperature

The reaction temperature was maintained at 15, 15 in dark, 37, 60°C in round bottom flask on hot plate magnetic stirrer and 15°C using shaking. Other optimization conditions were used, as followed previously.

7.2. Time

The time required for the reaction completion was monitored through 75 min, with time interval 15 min. Other optimization conditions were used, as followed previously.

7.3. *p*H

The *p*H of reaction was maintained at 4, 5, 6, 7, 8 and 9, respectively. Other optimization conditions were used, as followed previously.

7.4. Ratio of silver nitrate and the juice

The reaction was monitored by utilizing various proportion of $AgNO_3$ and juice solution (1:1, 2:1, 3:1, 4:1, 1:2, 1:3 and 1:4).

7.5. Concentration of $AgNO_3$ solution

The procedure mentioned was refined to optimization of $AgNO_3$ concentration; the reaction was maintained using various concentration of $AgNO_3$ (0.25, 0.5, 1, 2 and 4 mM), respectively. Other optimization conditions were used, as followed previously.

7.6. Stability of $AgNO_3$ solution

Stability of $AgNO_3$ was observed along with 48 h, for 30 days (at room temperature).

8. Characterization of AgNPs

8.1. UV-Vis spectrum analysis

Analysis of UV–Vis spectrum was done using (PG Instruments Limited, T80, Germany) spectrophotometer from 190 to 900 nm (1 nm resolution). The pure Ag^+ ions reduction was monitored by observing the spectrum at room temperature. Maximum absorbance of AgNPs showed at near 445 nm.

8.2. FTIR analysis

The biosynthesized AgNPs sample was treated as in previous work [13] and analyzed by FTIR (shimadzu-8400S) spectrophotometer, finally, compared the result with the spectrum of the extract.

8.3. AFM analysis

The biosynthesized AgNPs were characterized by Atomic Force Microscope (AFM) to identified the size distributions using (Model AA3000, Angstrom Advance Inc., USA) [14], [15].

8.4. SEM analysis

Shape, morphologies of biosynthesized AgNPs were characterized by Scanning electron microscopy (SEM), using (SEM-TeScan VEGA 3 SB, USA).

8.5. Zeta potential analysis

Zeta potential measurement was used to characterized the biosynthesized AgNPs. Zeta potential, size of NPs were measured by Electrophoretic Light Scattering (ELS) and Dynamic Light Scattering (DLS) using ZetaPlus (Brookhaven Instruments Corp., USA). The results were averaged with five time measurements.

8.6. Antimicrobial activity (well diffusion method)

The synthesized AgNPs by *Carica papaya* juice were analyzed for the antibacterial activity using well diffusion procedure against pathogenic organisms with *Escherichia coli* (*E. coli*), *Pseudomonas aurius* (*P. aureus*) *Klebsiella pneumonia* (*k. pneumoniae*) and *Staphylococcus aureus* (*S. aureus*). Using micropipette, the test samples (S1=AgNPs 3.47 ppm, S2=AgNPs 2 ppm, S3=AgNPs 1 ppm, S4=AgNPs 0.5 ppm, S5=$AgNO_3$ (1mM) 169.9 ppm and S6=Extract of *Carica papaya* juice) respectively, were prepared with serial dilution from stock one (S1=3.47 ppm, measured by AA spectroscopy) with deionized water and poured into wells on all plates [15], [16].

8.7. Effect of AgNPs on GOT and GPT activities

The glutamate oxaloacetate transaminase (GOT), glutamate pyruvate transaminase (GPT) activities were measured by the method of Reitman and Frankel using Randox Kit at 546 nm against the reagent blank.

A- The samples (S1=AgNPs 3.47 ppm, S2=AgNPs 2 ppm, S3=AgNPs 1 ppm, S4=AgNPs 0.5 ppm, S5=$AgNO_3$ (1mM) 169.9 ppm and S6=Extract of *Carica papaya* juice) respectively. The human serum GOT, GPT enzymes activities were measured by adding 100µl of sample (S1-S6) or deionized water (for blank). The inhibition percentage was calculated according to the equation:

$$\% \text{ Inhibition} = 100 - 100 \text{ X } \frac{\text{The activity with inhibitor}}{\text{The activity without inhibitor}}$$

B- The concentration of AgNPs (S2 – 2 ppm) was used to study the type of inhibition with different concentrations of substrate (40, 80, 120, 160, 200) mM for GOT, GPT. The activities of enzymes with and without AgNPs (S2) were determined and drawing 1/V against 1/[S] (Lineweaver-Burk equation) for measuring values:

A) Apparent (V_{max}^{app}), B) Apperent (K_m^{app}), C) Type of inhibition or activation.

RESULTS AND DISCUSSION

Phytochemical constituents of *Carica papaya* juice:

Qualitative chemical analysis of *Carica papaya* juice shown in Table-1, which indicated that juice contents were: glycosides, proteins, phenolic compounds, tannins, resins, flavonoids and alkaloids. Other studies showed that *Carica papaya* fruit is a good source of many components like provitamin a carotenoids, B vitamins, ascorbic acid, lycopene, fiber and minerals. Danielone (phytoalexin) detected in this fruit. *Carica papaya* has different phenolic groups act as scavenge free radicals [17]. The leaves and fruit of *Carica* papaya are rich in enzymes (hydrolytic proteins); act as a good antioxidant and an eminent antimicrobial agent [18-21]. Similar results were obtained by other studies which indicated the presence of carbohydrate, glycosides, proteins, phenolic compounds, alkaloids, terpenoids, flavonoids, saponins and steroids in *Carica papaya* Fruit juice [17, 22].

Table 1: Chemical components analysis (qualitative methods) of *Carica papaya* fruit juice.

Components	Reagents	Note	Result
Glycosides	Iodine test Molish test Benedict test	---- Purple ring Blue sol.	**_ve** **+ve** **+ve**
Phenolic compounds	Ferric chloride $FeCl_3$ 3%	Green ppt	**+ve**
Tannins	Ferric chloride $FeCl_3$ 3% Lead acetate 0.1%	Green ppt Yellow ppt	**+ve** **+ve**
Resins	Ethanol	Turbidity	**+ve**
Flavonoids	Ethanol+KoH	Yellow ppt	**+ve**
Alkaloids	Mayer's reagent Wagner reagent Picric acid	White ppt Brown ppt Yellow ppt	**+ve** **+ve** **+ve**

Table 2: The trace elements content of *Carica papaya* fruit juice.

Trace elements		Concentration ppm
Zinc	Zn	0.904
Cobalt	Co	0.272
Nickel	Ni	0.294
Cadmium	Cd	Nil
Iron	Fe	0.017
Manganese	Mn	0.16
Copper	Cu	0.124
Lead	Pb	Nil

Table 3: Retention time, name and molecular weight of *Carica papaya* fruit juice detected by GC-Mass

Peak	Peak Line	Name of the compound	Formula	Molecular Weight	Retention time
1	Line 1	Methanamine	C2H7NO	61	3.667
2		Glyceraldehyde	C3H6O3	90	
3		Ehtyl acetimidate	C4H9NO	87	
4		Glycerin	C3H8O3	92	
5	Line 2	3,5-Dihydroxy-6-methyl-2,3-dihydro-4H-pyran-4-one	C6H8O4	144	8.883
6		2,4,5-Trimethyl-1,3-dioxolane	C6H12O2	116	
7		Ethoxyethene	C4H8O	72	
8		1,2,4,5-Tetramethyl-1,2,4,5-tetraazinane	C6H16N4	144	
9		2,4-Dihydroxy-2,5-dimethyl-3(2H)-furanone	C6H8O4	144	
10	Line 3	Nitroisobutylglycerol	C4H9NO5	151	13.200
11		Butoxyacetic acid	C6H12O3	132	
12		Sucrose	C12H22O11	342	
13		Oxirane	C6H10O3	130	
14		Glycidyl butyl ether	C7H14O2	130	
15	Line 4	2-methyl-Hexanoic acid	C7H14O2	130	18.992
16		2-methyl-Pentanoic acid	C6H12O2	116	
17		Tetradecanoic acid	C16H32O2	256	
18		2-methyl-Undecanoic acid	C12H24O2	200	
19		Methyl dodecanoate	C13H26O2	214	
20	Line 5	Oxalic acid, butyl propyl ester	C9H16O4	188	22.250
21		Oxalic acid, isobutyl propyl ester	C9H16O4	188	
22		Diisobutyl 2-oxomalonate	C11H18O5	230	
23		1-Cyclopentyl-2,2-dimethyl-1-propanol	C10H20O	156	
24		1,1-Diisobutoxy-isobutane	C12H26O2	202	
25	Line 6	Glycidol methacrylate	C7H10O3	142	23.000
26		Vinyl methacrylate	C6H8O2	112	
27		Cyclopropyl ethyl ketone	C6H10O	98	
28		Allyl methacrylate	C7H10O2	126	
29		3,3-dimethyl-1,5-Heptadiene	C9H16	124	
30	Line 7	2,3,4-Trimethyl-1-pentanol	C8H18O	130	25.183
31		3,3,4-Trimethyldecane	C13H28	184	
32		3,4-Diethyl hexane	C10H22	142	
33		3-Ethyl-4-methylheptane	C10H22	142	
34		Isopentyl ether	C10H22O	158	
35	Line 8	3,3,4-Trimethyl-1-decene	C13H26	182	26.958
36		(5E)-3-Methyl-5-undecene	C12H24	168	
37		2-Ethylhexyl methacrylate	C12H22O2	198	
38		3,4-Diethyl hexane	C10H22	142	
39		(2Z)-3-Methyl-2-undecene	C12H24	168	

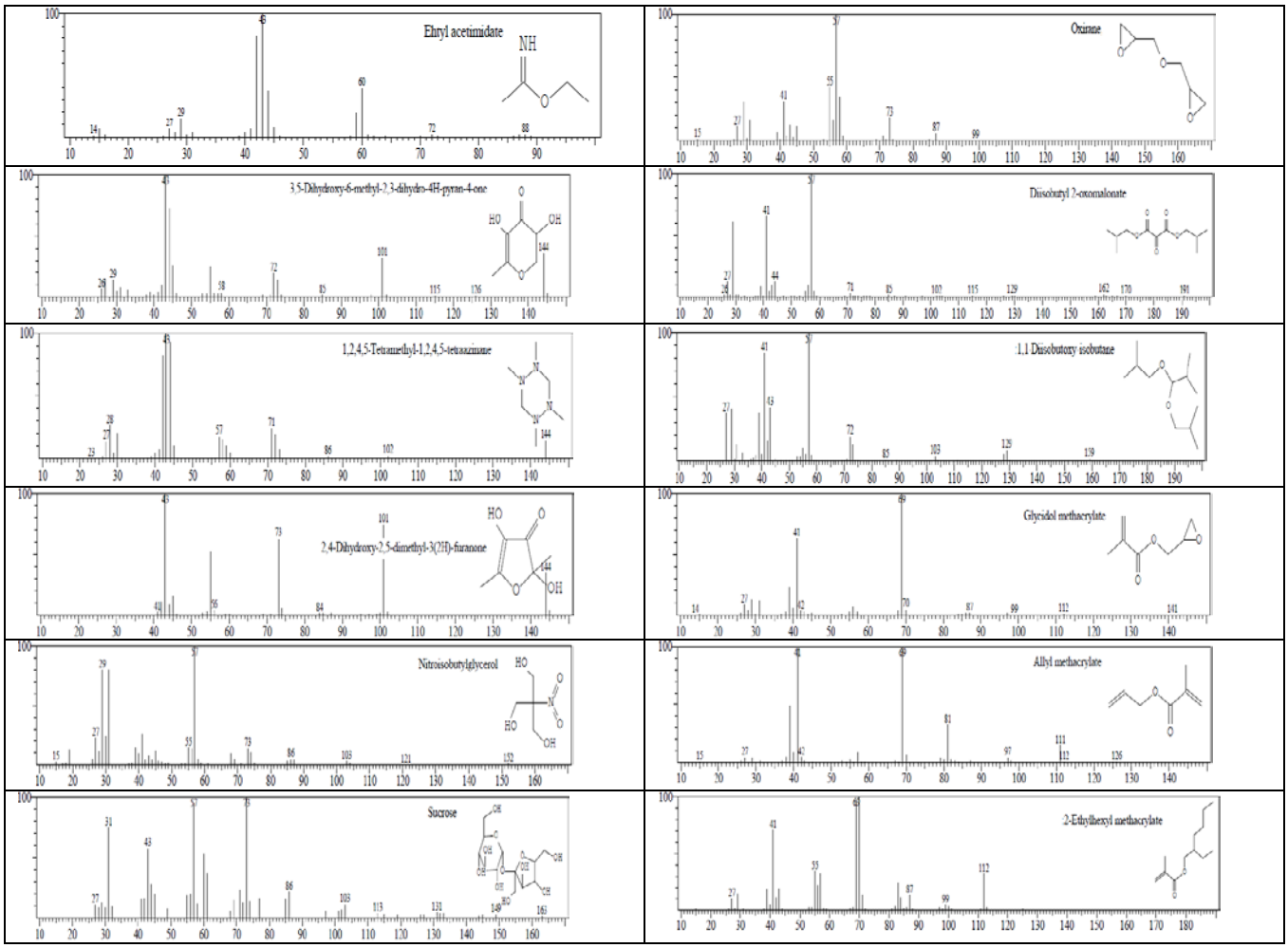

Fig 2: GC-Mass Spectrum of the main compounds identified in *Carica papaya* fruit juice

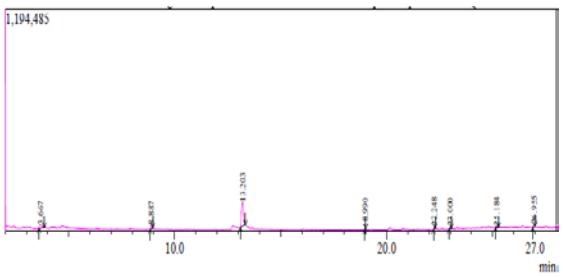

Fig1. The chromatogram of *Carica papaya* fruit juice detected by GC-Mass

The trace elements in *Carica papaya* fruit juice shown in Table-2, which indicated that the concentrations of (Zn, Co, Ni, Fe, Mn and Cu) were (0.904, 0.272, 0.294, 0.017, 0.160, 0.124) ppm, respectively, and both of (Cd and pb) were not detected. Many other researchers indicated the presence of different minerals found in this plant [17, 22].

A study of ethyl acetate fraction by GC-Mass to *Carica papaya* fruit juice has shown many compounds (Figure 1 and Tables 1) with different groups like CO, NO, OH, COOH, NH…*etc*, which participate in reducing power of this plant and acting as capping and reducing agent to synthesis AgNPs. The main compounds identified in fruit juice were shown in Figure 2. It is clear from Table 3 that some components have complex chemical structures. The results clearly illustrate that the fruit juice was rich in phenolic compounds, carboxlic acids, aldehydes, antioxidants, unsaturated fatty acids, terpenes and others [13].

Biosynthesis of AgNPs:

Green synthesis by using plants is stocked with different metabolites that are capable of reducing metal salts to form many types of NPs. The silver ions in aqueous form were reduced to AgNPs when added to *Carica papaya* fruit juice. Alteration in color of mixture solution, yellow to bright yellow to brown, was seen gradually, which indicated to AgNPs formation (Figure 3).

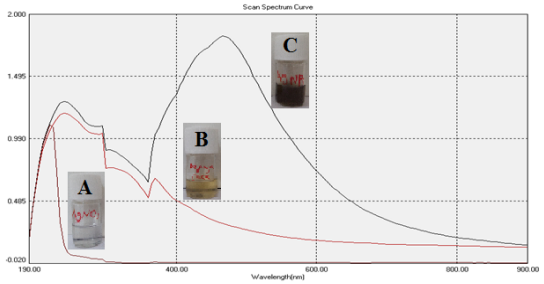

Fig 3: UV–Vis spectra and color change in reaction mixture of A-Aqueous solution of 1mM AgNO3, B-*Carica papaya* fruit juice, C- AgNPs.

The formation and stability of the colloidal AgNPs was monitored by UV–Vis spectrum, which showed a maximum absorbance near 445 nm, elevated with time of incubation of $AgNO_3$ with the *Carica papaya* juice. The above curve shows increasing absorbance with time intervals. The peaks were noticed near 440-450nm belongs to the surface plasmon resonance (SPR) of AgNPs. The data indicated that the reduction of the sliver ions took place extra-cellularly and broadening of peak clarified that the synthesized particles are poly-dispersed [23].

Fixation of various parameters:

Various parameters were optimized and characterized as affecting agents on the yields of AgNPs:

A- Temperature:

As shown in figure 4, the producing rate of AgNPs increased, when temperature elevated. The size at the beginning of reaction was decreased because of reduction in aggregation of the growing AgNPs. Elevating temperature near (60°C) assist the crystal developments surround the nucleus. Furthermore, the color change during this reaction after (15, 30, 45, 60 min) shown in (Figure 5).

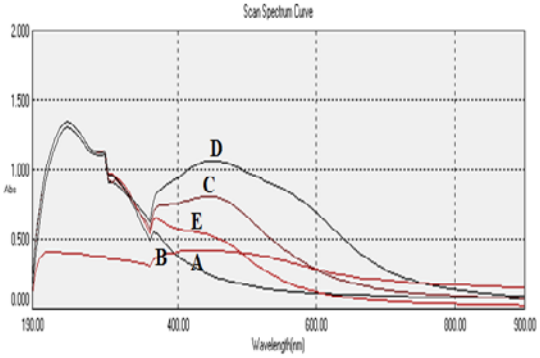

Fig 4: UV–Vis spectra for different temperature (A=15°C, B=15°C in dark, C=37°C, D=60°C on stirring hot plate and E=15°C using shaking)

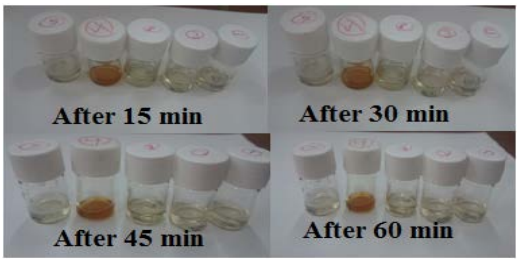

Fig 5: Color change for different temperature (15, 30, 45, 60 min).

B- Time:

The other factor considered was the reaction time required. The results showed gradual elevating of absorbance spectrum as the reaction time increasing with SPR near 435 nm, so color intensity elevated concurrent with incubation, which indicated the increasing in AgNPs formation. Our Study indicated that the time required to complete the formation of AgNPs was 60 min (Figure 6) and the color change during this reaction shown in (Figure 7). As compared with previous studies, the time required for reduction of Ag ions ranged from 60 min [23] to 48 h or even more than one week [24].

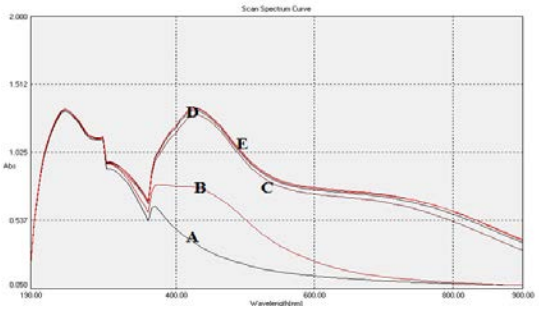

Fig 6: UV–Vis spectra for different time A=15 min, B=30 min, C=45 min, D=60min, E=75 min) temperature 60°C.

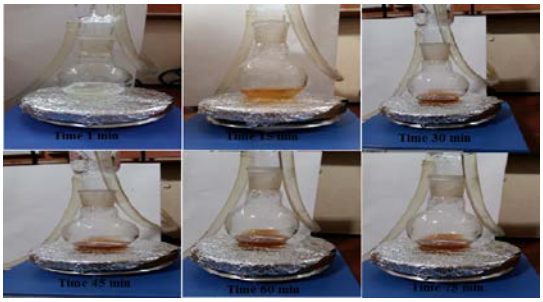

Fig 7: Color change for different time (1, 15, 30, 45, 60, 75 min).

C- *p*H:

The effect of *p*H on formation of AgNPs was shown in Figure 8, while Figure 9 shows the color change during this reaction. There can be seen that elevated in absorbance associated with elevated in *p*H (4 to 7) while it has been decreased with 8 and 9. So, it was found that the optimum *p*H for the reaction was 6. The same results were shown in our previous study [13], as well as others researcher, Veersamy *et al*. [23] and Khalil *et al*. [24]. These studies confirmed that shape and size of synthesized AgNPs could be influenced by changing of *p*H media which leads to change the electrical charges of bio-components work as capping and stabilizing agents.

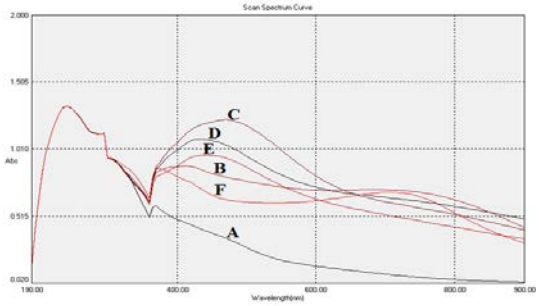

Fig 8: UV–Vis spectra for different *p*H (A=4, B=5, C=6, D=7, E=8, F=9) temperature=60°C, time=60 min.

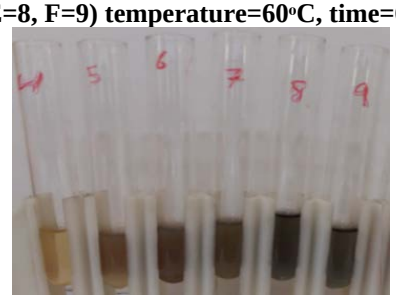

Fig 9: Color change for different *p*H (from left to right A=4, B=5, C=6, D=7, E=8, F=9)

D- Ratio of silver nitrate and fruit juice:

Optimization of $AgNO_3$ and *Carica papaya* fruit juice desired for extreme production of AgNPs, were monitored by changing the ratio of $AgNO_3$ and the fruit juice (Figure 10). The data showed that the best ratio was 3:1 depends on the optimum absorbance and number of trials. The color changed during this reaction shown in Figure 11.

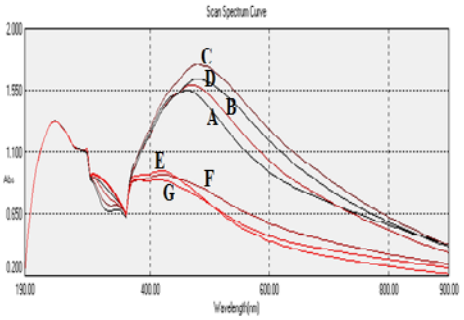

Fig 10: UV–Vis spectra for different ratio of AgNO3 and the fruit juice (A=1:1, B=2:1, C=3:1, D=4:1, E=1:2, F=1:3 and G=1:4) temperature=60°C, time=60 min, *p*H=6.

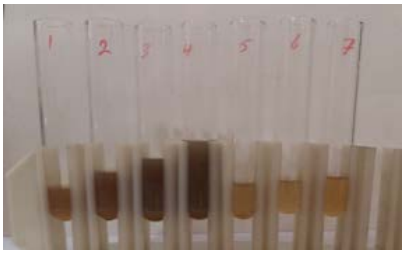

Fig 11: Color change for different ratio of $AgNO_3$ and the fruit juice (from left to right A=1:1, B=2:1, C=3:1, D=4:1, E=1:2, F=1:3 and G=1:4)

E- Concentration of $AgNO_3$ solution:

The other factor was the concentration of $AgNO_3$. Different concentrations of $AgNO_3$ solution were used to get extreme production of AgNPs. The data showed that the best production with 1 mM of $AgNO_3$ (Figure 12) and the color change during this reaction shown in (Figure 13). Whenever the $AgNO_3$ increased, the adversity of yellow color developed to deep brown. Increasing the $AgNO_3$ concentration made the SPR peak featured [25]. So, to achieve control of growth and smaller particle size, the above mentioned conditions have been used for the further study.

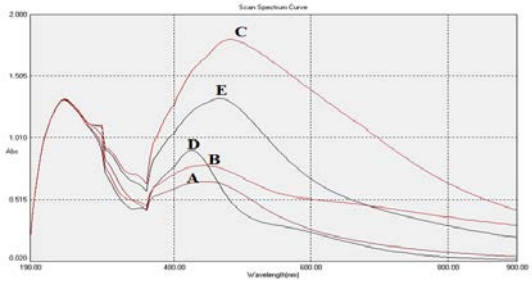

Fig 12: UV–Vis spectra for different concentration of $AgNO_3$ (A=0.25, B=0.5, C=1, D=2 and E=4 mM) temperature=60°C, time=60 min, *p*H=6, ratio 3:1

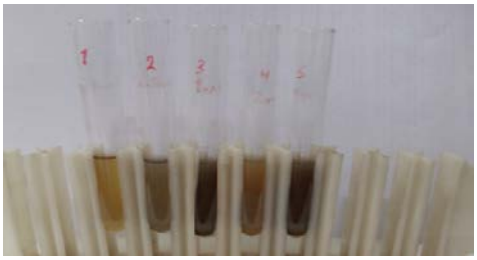

Fig 13: Color change for different concentration of $AgNO_3$ (from left to right A=0.25, B=0.5, C=1, D=2 and E=4 mM)

The overall optimized reaction conditions were: temperature=60°C, time=60 min, *p*H=6-7 (weak acidic to neutral), the concentration ratio of $AgNO_3$ to the *Carica papaya* juice=3 : 1, and concentration of $AgNO_3$=1 mM. The prepared AgNPs were steady for one month near 25°C (Figure 14).

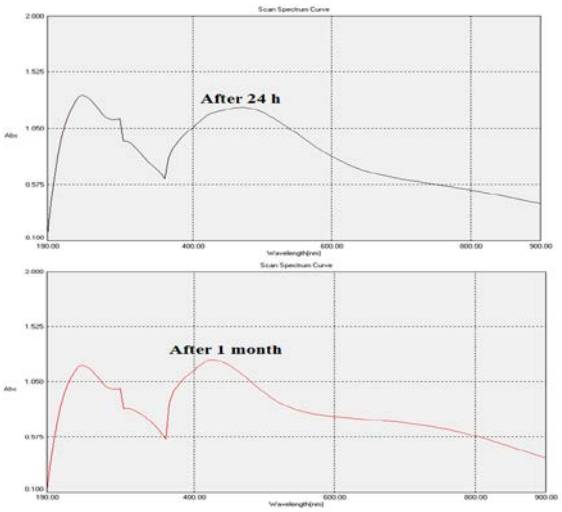

Fig 14: UV–Vis spectra of prepared AgNPs after 24h and after 1 month.

FTIR analysis:

The FTIR analysis was achieved to characterize the prospective bio-molecules responsible to formation of AgNPs by reduction of silver ions to Ag^o and its stabilization as capping agent. The spectra of *Carica papaya* fruit juice and AgNPs produced (after reaction with $AgNO_3$) have been shown in (Figure 15, A & B), respectively. It can be seen a characteristic bands belong to AgNPs identical to those of *Carica papaya* fruit juice, which indicating that AgNPs were coated with the bio-molecules of the extracts.

The bands near 684 and 667 cm^{-1} is assigned to CH out of plane of substituted ethylene systems –CH=CH. The bands at 1049, 1055 cm^{-1} belong to C-OH stretching of secondary alcohols. Broad peaks between 3201-3448 and 3184-3277 $cm^{-1}$for *Carica papaya* fruit juice and AgNPs, respectively, belong to -NH stretching in amide (II) or bending of –O–H stretching. In NPs, a high shift in the peak with low intensity was observed from 3201-3448 to 3184-3277 and 1417 to 1410 cm^{-1}, with disappear peak at 1350 cm−1, implying the binding of silver ions with hydroxyl, N–H of amines and carboxylate groups of the extract to stable

AgNPs [26, 28]. Band at 2933 cm^{-1} belongs to asymmetric stretching of C-H groups [27].

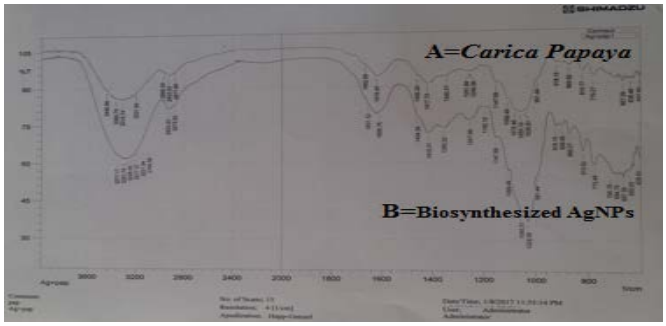

Fig 15: FTIR spectra of (A) *Carica papaya* fruit juice and (B) synthesized AgNPs.

The *Carica papaya* is an affluent origin of medicinally important components like proteins, carbohydrate, minerals, vitamins and phenolic components, alkaloids and others [18-21]. The FTIR confirmed the data shown by GC-Mass, that the fruit juice included important groups as OH, CO, NO, COOH, NH act in capping the NPs synthesis and might be contribute to stability.

AFM analysis

Identifying the size and morphology of AgNPs was down by AFM analysis. The surface morphology of the particles sizes with irregularly shaped and the size distribution of AgNPs synthesized by *Carica papaya* fruit juice were shown in Figure 16, with average size diameter 75.68 nm.

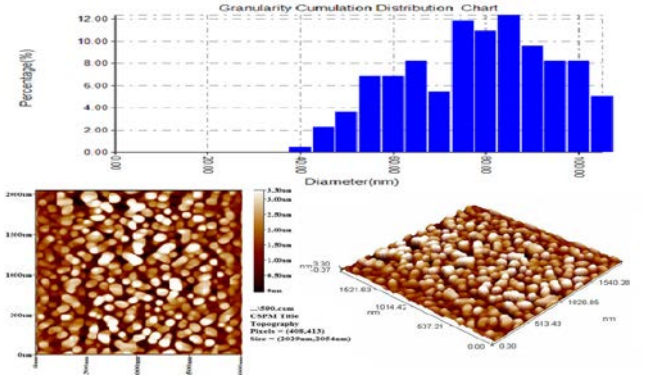

Fig 16: AFM images (2D & 3D) and size distributions of synthesized AgNPs

The SEM (Figure 17, A-D) was identifying the structure and morphology of the NPs. The data showed relatively spherical shape NPs with coated materials from *Carica papaya* fruit juice and a diameter ranging near to 500 nm (as shown later by Zeta potential). The relatively spherical shaped AgNPs with a different diameter range using SEM which synthesized using *Boswellia* [28]; using *Shorea tumbuggaia* [29]; plant extracts of *Aloe vera* [30]; *Carica papaya* [31] and with orange peel extract [32].

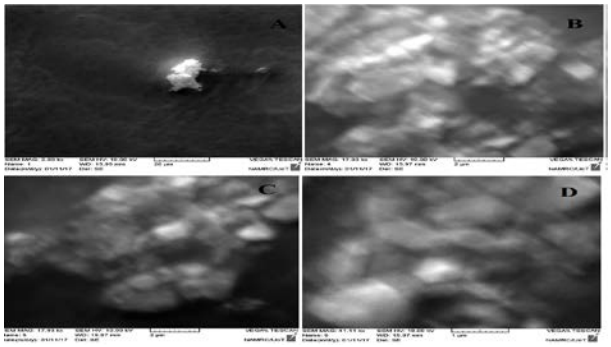

Fig 17: SEM images of synthesized AgNPs (A=20µm, B=2µm, C=2µm, D=1µm)

Zeta potential analysis:

Zeta potential distribution of synthesized AgNPs was measured by Electrophoretic Light Scattering (ELS) equal to –16.93 mV (n = 5), and the mobility (µ/s) / (V/cm) of the sample was –1.32 as shown in Figure 18. The ELS is originally used for identifying the surface charges of colloidal particles or other macromolecules in liquid media in an electric field [33]. The ELS can identify different particle size for proteins and gives information about surface charges [34].

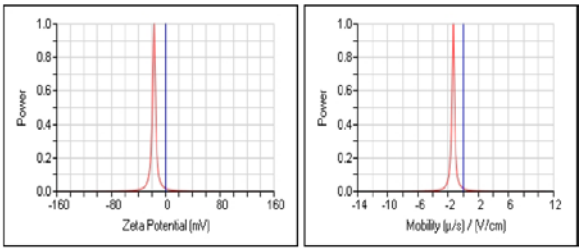

Fig 18: Zeta potential distribution, mV (left) and mobility (µ/s) / (V/cm), of synthesized AgNPs

The effective diameter and polydispersity of synthesized AgNPs measured by (DLS) equal to 555.21 nm 0.330, respectively, as shown in Figure 19. The charge and particle surface feature play the important action in the particle's physical state, agglomeration tendencies, stability in diverse reaction and interaction with biological media [35]. The stability at minimal zeta potential more commonly implies some degree of steric stabilization. So, these results obviously shown that the particles in solution are less stable (relatively) due to the zeta potential was less than ±30 mV.

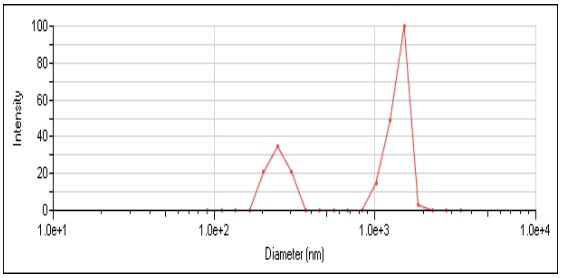

Fig 19: The effective diameter (nm) and Multimodal Size Distribution of synthesized AgNPs

The NPs need a suitable functional group on the surface to conjugating with different bio-molecules. Most bio-molecules have a primary amine, phosphate, carboxylic acid, thiol or an alcohol group on their surfaces [13, 36-38] and different one of these components can be interact with surface of NPs in order to surrounding the NPs as illustrated in Figure 20.

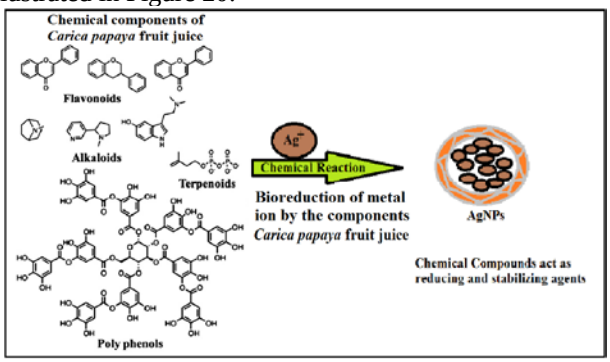

Fig 20: Possible compounds of *Carica papaya* fruit juice responsible for bioreduction of AgNPs.

Furthermore, the mechanism of AgNPs synthesized by plant extracts involved three main steps: (1) Activation step (2) Growth step (3) Termination step to form the final shape of the NPs [39] as illustrated in Figure 21.

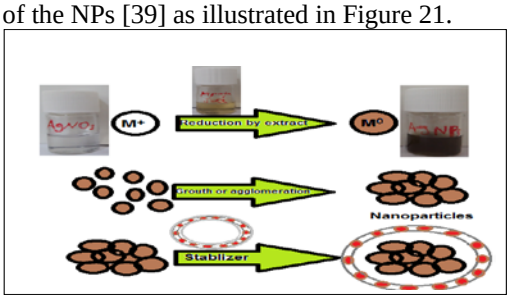

Fig 21: Proposed mechanisms to synthesis AgNPs by using *Carica papaya* fruit juice as reducing and stabilizing agent (M^+-metal ion).

Antimicrobial activity:

The AgNPs concentration equal to 3.47 ppm (S1), which measured by AAS. The Figure 22 and Figure 23 showed the inhibition zone on nutrient agar by well diffusion method using *E. coli*, *P. aureus*, *k. pneumoniae* and *S. aureus* as a function of AgNPs concentrations (S1-S4), $AgNO_3$ (S5) and *Carica papaya* fruit juice (S6). The results indicated that the bacteria were inhibited by different concentrations used.

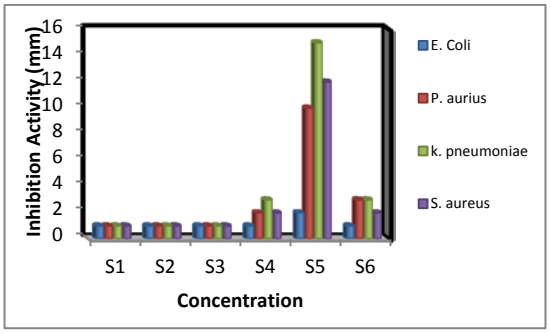

Fig 22: Inhibition activity of AgNPs (S1-S4), $AgNO_3$ (S5) and *Carica papaya* fruit juice (S6) against *E. coli, P. aureus, k. pneumoniae* and *S. aureus*.

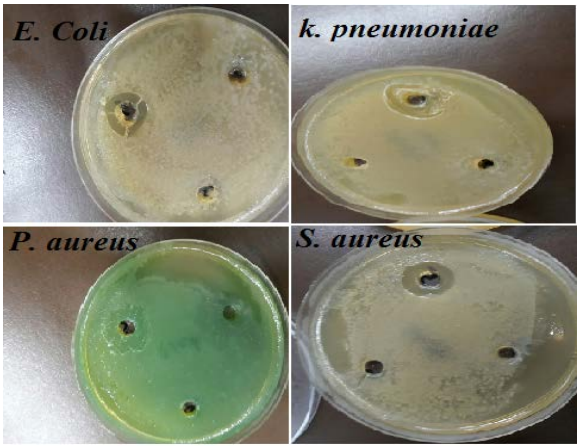

Fig 23: Antibacterial Activity of AgNPs (S1-S4), $AgNO_3$ (S5) and *Carica papaya* fruit juice (S6) using *E. coli, P. aureus, k. pneumoniae* and *S. aureus*

The *E. coli* was less sensitive to AgNPs as compared to *S. aureus*, this was in agreement with other works [13, 24], while Kim *et al*. [40] showed that *S. aureus* was less affected by AgNPs compared with *E. Coli* even in high concentrations (reverse to our results. Furthermore, the highest assay of inhibition was achieved for *k. pneumonia*, when the lowest concentration of (S4) and (S6) were used.

The effect of AgNPs on GOT and GPT activities:

This research investigates the AgNPs effects on GOT and GPT enzymes. The biochemical study illustrated that AgNPs caused inhibitory effects to these enzymes. Our results indicate that the concentration of AgNPs (S2) inhibited both of enzymes with (76.5 %) and (73.9 %) as shown in Figure 24 A and B, respectively.

The results in Table 4 and Figure 25A, showed the kinetic parameters (V*max*, K*m* and inhibition type) for AgNPs on serum GOT activity using Lineweaver-Burk plot. The values of Vmax, Km without AgNPs were 16.67 U/L and 58.8 mM, respectively. A liquate concentration 2 ppm of AgNPs (S2) was competitive inhibition to GOT, which changed the K*m* without V*max* of the enzyme. When AgNPs-S2 used, the V_{max}^{app} and K_m^{app} were 16.67 U/L, 80 mM, respectively.

The results in Table 4 and Figure 25B, showed the kinetic parameters (V*max*, K*m* and inhibition type) for AgNPs on serum GPT activity using Lineweaver-Burk plot. The values of V*max*, K*m* without AgNPs were 15.38 U/L, 90.9 mM, respectively. A liquate concentration 2 ppm of AgNPs (S2) was competitive inhibition to GPT, which changed the K*m* without V*max* of the enzyme. When AgNPs-S2 used, the V_{max}^{app} and K_m^{app} were 15.38 U/L, 333.3 mM, respectively. Our previous study indicated the effect of biosynthesized AgNPs on these enzymes [13].

Table 4: kinetic properties of GOT and GPT with AgNPs

Enzyme	V_{max} U/L	K_m mM	$\mathbf{V_{max}^{app}}$ U/L	$\mathbf{K_m^{app}}$ mM	Inhibition type
GOT	16.67	58.8	16.67	80	Competitive
GPT	15.38	90.9	15.38	333.3	Competitive

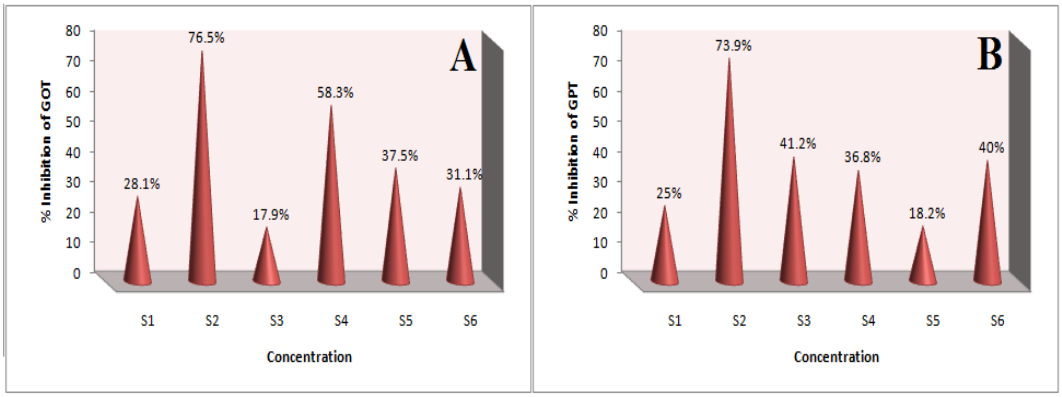

Fig 24: Percentage Inhibition of GOT (A) and GPT (B) by AgNPs (S1-S4), $AgNO_3$ (S5) and *Carica papaya* fruit juice (S6)

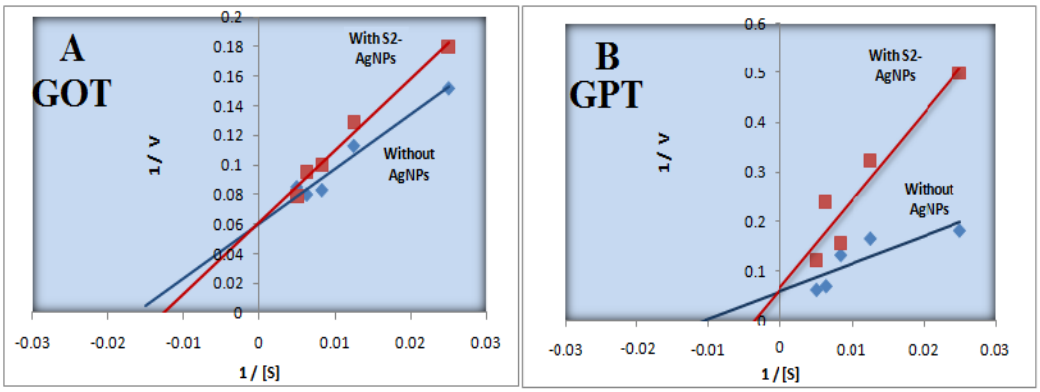

Fig 25: Lineweaver-Burk plots of AgNPs (S2) on the GOT (A) and GPT (B)

The heavy metals are toxic and can react with proteins; which strongly interact to thiol portion in enzymes to inactivate them. Also, silver and gold bind to these proteins (or enzymes), made protein deactivation and denaturation [41]. We hypothesized that NPs of AgNPs interact with GOT and GPT, resulting in protein denaturation or inactivate it, so this AgNPs inhibited these enzymes.

CONCLUSION

The *C. papaya* fruit juice has beneficial properties for health and therapy. The *C. Papaya* fruit juice capable of synthesized AgNPs and work as both reducing and stabilizing agent because this fruit juice contains many components which analyzed by GC-Mass. The synthesized NPs were confirmed by UV–Vis, FTIR, AFM, AA, SEM, and Zitasizer. Color changes were produced at optimal conditions. The rate of formation of the AgNPs increased significantly in weak acidic to neutral medium with increasing temperature. The *C. Papaya* can produce useable NPs. which can be utilized for antibacterial applications and have effective role against liver enzymes.

Acknowledgements

The authors thank Mustansiriyah University, Baghdad, Iraq (www.uomustansiriyah.edu.iq) for their helpful to accomplish this work.

REFERENCES

[1] Timothy, V. D. Applications of Nanotechnology in Food Packaging and Food Safety: Barrier Materials, Antimicrobials and Sensors. *J. Colloid and Interface Sci.* **2011**, *363*, 1-24.

[2] Stanley Rosarin, F. S.; Mirunalini Nobel Metallic Nanoparticles with Novel Biomedical Properties. *J. Bioanal. Biomed.* **2011**, *3(4)*, 85-91.

[3] Singh M. S.; Manikandan ; Kumaraguru, A. K. Nanoparticles: A New Technology with Wide Applications *Res. J. Nanosci. Nanotechnol.* **2010**, *10*, 1996-2014.

[4] Ip M.; Lui, S. L.; Poon, V. K. M.; Lung, I.; Burd, A. Antimicrobial Activities of Silver Dressings: An *In Vitro* Comparison. *J. Medical Microbial.* **2006**, *55*, 59-63.

[5] Awad M. A.; Hendi, A. A.; Ortashi, K. M. O.; Elradi, D. F. A.; Eisa, N. E.; Al-lahieb, L. A.; Al-Otiby, S. M.; Merghani, N. M.; Awad, A.A.G. Silver Nanoparticles Biogenic Synthesized Using an Orange Peel Extract and Their Use As an Anti-bacterial Agent. *International journal of physical science* **2014**, *9 (3)*, 34-40.

[6] Maham M.; Nasrollahzadeh M.; Sajadi S. M.; Nekoei M. Biosynthesis of Ag/Reduced Graphene Oxide/Fe3O4 Using *Lotus Garcinii* Leaf Extract and Its Application As a Recyclable Nanocatalyst for The Reduction of 4-Nitrophenol and Organic Dyes. *Journal of Colloid and Interface Science* **2017**, *497*,33–42

[7] Njagi E. C.; Huang, H.; Stafford, L.; Genuino, H.; Galindo, H. M.; Collins, J. B.; Hoag, G. E.; Suib, S. L. Biosynthesis of Iron and Silver Nanoparticles at Room Temperature Using Aqueous Sorghum Bran Extracts. *Langmuir* **2011**, *27(1)*, 264–271.

[8] Aravind, G.; Debjit, B.; Duraivel, S.; Harish, G. Traditional and Medicinal Uses of *Carica Papaya*. *J. Med. Plants Stud.* 2013, *1 (1)*, 7–15.

[9] Sinhalagoda, L. C. A. D.; Susiji, W.; Roshitha, N. W.; Rajapakse, P. V. J. R.; Senanayake, A. M. K. Does *Carica papaya* Leaf Extract Increase the Platelet Count? An Experimental Study in a Murine Model. *Asian Pac. J. Trop. Biomed*. **2013**, *3 (9)*, 720–724.

[10] Kadry, M. S. Antioxidant And Immunostimulant Effect of *Carica papaya* Linn Aqueous Extract in Acrylamide Intoxicated Rats. *Acta Inform. Med*. **2012**, *20 (3)*, 180–185.
[11] Banala R. R.; Nagati V. B.; Karnati P. R. Green Synthesis and Characterization of *Carica papaya* Leaf Extract Coated Silver Nanoparticles Through X-Ray Diffraction, Electron Microscopy And Evaluation of Bactericidal Properties. *Saudi Journal of Biological Sciences* **2015**, *22*, 637–644.
[12] Farhan S. A.; Faraj M.; Al-Shemari H. H.; Jassim A. M. N. Study of Some *Urtica dioica* L. Leaves Components and Effect of Their Extracts on Growth of Pathogenic Bacteria and Identify of Some Flavonoids by HPLC. *Al- Mustansiriya J. Sci.* **2012**, *23(3)*, 79-86.
[13] Jassim A. M. N.; Farhan S. A.; Dadoosh R. M. Green Synthesis of Silver Nanoparticles Using Seed Aqueous Extract of *Abelmoschus Esculentus* and Study of Their Properties. *Advances in Environmental Biology* **2016**, *10(4)*, 51-66.
[14] Bigall N. C.; Eychmuller, A. Synthesis of Noble Metal Nanoparticles and Their Non-ordered Superstructures. *Phil. Trans. R. Soc. A.* **2010**, *368*, 1385-1404.
[15] Jassim, A. M. N.; Farhan, S. A.; Salman, J. A. S.; Khalaf, K. J.; Al-Marjani, M. F.; Mohammed, M. T. Study the Antibacterial Effect of Bismuth Oxide and Tellurium Nanoparticles. *International Journal of Chemical and Biomolecular Science* **2015**, *1(3)*, 81-84.
[16] Tomi, I. H. R.; Al-Daraji, A. H. R.; Abdula, A. M.; Al-Marjani M. F. Synthesis, Antimicrobial and Docking Study of Three Novel 2,4,5-Triarylimidazole Derivatives. *Journal of Saudi chemical society* **2016**, *20*, s509-s516.
[17] Aravind G.; Debjit B.; Duraivel S.; Harish G. Traditional and Medicinal Uses of *Carica papaya*. *Journal of Medicinal Plants Studies* **2013**, *1*(*1*), 7-15.
[18] Zuhair, R. A.; Aminah, A.; Sahilah, A.M.; Eqbal, D. Antioxidant Activity and Physicochemical Properties Changes of Papaya (*Carica papaya* L. cv. Hong Kong) During Different Ripening Stage. *Int. Food Res. J*. **2013**, *20 (4)*, 1653–1659.
[19] Zuhair, R. A.; Aminah, A.; Sahilah, A. M.; Khalid, H. M.; Eqbal, M.A.D. Antioxidant Activity and Physicochemical Properties of Mature Papaya Fruit (*Carica papaya* L. cv. Eksotika). *Advance. J. Food Sci. Technol.* **2013**, *5 (7)*, 859–865.
[20] Maisarah, A. M.; Amira, B. N.; Asmah, R.; Fauziah, O. Antioxidant Analysis of Different Parts of *Carica papaya*. *Int. Food Res. J.* **2013**, *20 (3)*, 1043–1048.
[21] Özkan, A.; Gübbük, H.; Güneş, E.; Erdoğan, A. Antioxidant Capacity of Juice from Different Papaya (*Carica papaya* L.) Cultivars Grown under Greenhouse Conditions in Turkey. *Turk. J. Biol*. **2001**. *35*, 619–625.
[22] Krishna, K. L.; Paridhavi, M.; Patel; Jagruti A. Review on Nutritional, Medicinal and Pharmacological Properties of Papaya (*Carica papaya* Linn.). *Natural Product Radiance* **2008**, *7 (4)*, 364-373.
[23] Veerasamy, R.; Zi Xin, T.; Gunasagaran, S.; Xiang, T. F. W.; Yang, E. F. C. ; Jeyakumar, N. ; Dhanaraj, S.A. Biosynthesis of Silver Nanoparticles Using Mangosteen Leaf Extract and Evaluation of Their Antimicrobial Activities. *Journal of Saudi Chemical Society* **2011**, *15*, 113-120.
[24] Khalil, M. M. H.; Ismail, E. H.; El-Baghdady, K. Z.; Mohamed, D. Green Synthesis of Silver Nanoparticles Using Olive Leaf Extract and Its Antibacterial Activity. *Arabian Journal of Chemistry* **2014**, 7, 1131–1139
[25] Iravani, S. Green Synthesis of Metal Nanoparticles Using Plants. *Green Chem.* **2011**, *13*, 2638–2650
[26] Banerjee, S. S.; Someshwar, S.; Subrata, L.; Chandra, G. Efficacy of *Limonia acidissima* L. (Rutaceae) Leaf Extract on Larval Immatures of Culexquinquefasciatus Say 1823. *Asian Pacific Journal of Tropical Medicine* **2011**, *4*, 711–716.
[27] Jayaseelana, C.; Ramkumar, R.; Rahuman A. A.; Perumal, P. Green Synthesis of Gold Nanoparticles Using Seed Aqueous Extract of *Abelmoschus Esculentus* and Its Antifungal Activity, *Industrial Crops and Products* **2013**, *45*, 423-429.
[28] Ankanna, S.; Prasad, T. N. V. K. V.; Elumalai E. K.; Savithramma, N. Production of Biogenic Silver Nanoparticles Using *Boswellia Ovalifoliata* Stem Bark. *Dig. J. Nanomater. Biostruct.* **2010**, 5, 369-372.
[29] Savithramma, N.; Rao M. L.; Suvarnalatha Devi, P. Evaluation of Antibacterial Efficacy of Biologically Synthesized Silver Nanoparticles Using Stem Barks of *Boswellia Ovalifoliolata* Bal. and Henry and *Shorea Tumbuggaia* Ruxb. *Journal of Biological Science* **2011**, *11*, 39-45.
[30] Chandran, S.P.; Chaudhary, M.; Pasricha, R. Ahmad, A.; Sastry, M. Synthesis of Gold Nanoparticles and Silver Nanoparticles Using *Aloe Vera* Plant Extracts. *Biotechnol. Prog.* **2006**, *22*, 577-583.
[31] Jain, D.; Daima, H.K.; Kachnwaha S.; Kothari, S.L. Synthesis of Plant Mediated Silver Nanoparticles Using Papaya fruit Extract and Evaluation of Their Antimicrobial Activities. *Dig. J. Nanomater. Biostruct.* 2009, 4, 723-727.
[32] Awad, M. A.; Hendi, A. A.; Ortashi, K. M. O.; Elradi, D. F. A.; Eisa, N. E.; Al-lahieb, L. A.; Al-Otiby, S. M.; Merghani N. M.; Awad, A. A. G. Silver Nanoparticles Biogenic Synthesized Using an Orange Peel Extract and Their Use As an Anti-Bacterial Agent. *Int. J. Phys. Sci.* **2014**, *9(3)*, 34-40.
[33] Okubo, T; Suda M. Absorption of Polyelectrolytes on Colloidal Surfaces as Studied by Electrophoretic and Dynamic Light-Scattering Techniques. *Journal of colloid and interface science* **1999**, *213(2)*, 565-571.
[34] Boevé, E. R.; Cao, L. C.; De Bruijn, W. C.; Robertson, W. G.; Romijn J. C.; Schröder, F. H. Zeta Potential Distribution on Calcium Oxalate Crystal and Tamm-Horsfall Protein Surface Analyzed with Doppler Electrophoretic Light Scattering. *The Journal of urology* **1994**, 152 *(2 Part 1)*, 531-536.
[35] Berg, J.M.; Romoser, A.; Banerjee, N.; Zebda, R.; Sayes, C.M. The Relationship Between *p*H and Zeta Potential of 30 nm Metal Oxide nanoparticle suspensions relevant to in vitro toxicological evaluations. *Nanotoxicology* **2009**, *3*, 276-283
[36] Marie-Alexandra N.; Schubert, I. Surface Modification, Functionalization of Metal and metal Oxide Nanoparticles by Organic Ligands. *Monatsh. Chem.* **2008**, 139, 183-195.
[37] Gref, R.; Couvreur, P.; Barratt, G.; Mysiakine, E. Surface-Engineered Nanoparticles for Multiple Ligand Coupling. *Biomaterials* 2003, *24*, 4529-4537.
[38] Ravindran, A.; Chandran P.; Khan, S. S. Biofunctionalized Silver Nanoparticles: Advances and Prospects. *Colloids and Surfaces B: Biointerfaces* **2013**, *105*, 342-352.
[39] Makarov, V. V.; Love, A. J.; Sinitsyna, O. V.; Makarova, S. S. ; Yaminsky, I. V.; Taliansky, M. E.; Kalinina, N. O. Green Nanotechnologies: Synthesis of Metal Nanoparticles Using Plants. *Acta naturae* **2014**, *6(1)*, 35-44.
[40] Kim, J.S.; Kuk, E.; Yu, K. N. ; Kim, J. H.; Park, S.J.; Lee, H.J.; Kim, S.H., Park, Y.K.; Park, Y.H.; Hwang, C.Y.; Kim, Y.K.; Lee, Y.S.; Jeong, D.H.; Cho, M.H. Antimicrobial Effects of Silver Nanoparticles. *Nanomed.: Nanotechnol. Biol. Med.* **2007**, *3*, 95-10.
[41] Abdullah, A.H.; Abbas, S. A. R.; Abdul Sada S. H.; Ali, K. A. The Effect of Gold and Silver Nanoparticles on Transaminase Enzymes Activities, *Int. J. Chem. Res*. **2011**, *1(4)*, 1-11.